

# Effect of Talc Size on Surface Roughness and Glossiness of Polypropylene Injection Molding Application to Automotive Plastics

Shinichi Kuroda <sup>1</sup>, Atsushi Mizutani,<sup>1</sup> Hiroshi Ito<sup>2</sup>

<sup>1</sup>Nissan Motor Co., Ltd, 1 Natsushima, Yokosuka, Kanagawa 237-8523, Japan

<sup>2</sup>Department of Organic Materials Science, Graduate School of Organic Materials Science, Yamagata University, 4-3-16 Jonan, Yonezawa, Yamagata 992-8510, Japan

**Talc-containing polypropylene (PP) resin is extensively employed in automobiles. Herein, considering the microstructure transfer process in injection molding, the effect of the talc's dispersibility and particle size on this process and its impact on the gloss level of the product were investigated. Results show that a fine unevenness of about several micrometers was self-formed by the shrinkage of PP in nontransferred areas due to the blending of talc. Additionally, the amount of self-formed unevenness tended with an increase in the average particle size of talc. Furthermore, due to PP shrinkage and different densities of talc, it was observed that a fine tiger-stripe pattern was self-formed using special molds with modified microstructure. This self-formed fine unevenness changes the gloss level owing to the diffused light reflection effect. This study proposes controlling this change by controlling the average particle size of talc and structure of the mold. POLYM. ENG. SCI., 00:000–000, 2019. © 2019 Society of Plastics Engineers**

## INTRODUCTION

Polypropylene (PP) is widely applied as a resin material in automobiles. Nomura et al. improved the PP performance by developing the polymer alloys that improved the performance of conventional PP and created PP that simultaneously exhibited high fluidity, high rigidity, and high impact resistance [1]. This was done based on the unique idea of sea-island conversion. Furthermore, they promoted the high crystallization and low-molecular weight of PP and succeeded in obtaining ultrafine PP crystals using a PP-compatible elastomer copolymer. In comparison with conventional products, the developed PP significantly improved the strength enhancing effect due to talc compounding. Even in recently developed resin materials for automobiles, several representative resin parts, such as bumpers or instrument members, often use PP containing approximately 10%–20% of talc or rubber using this technology. Polymerization and blending technologies are constantly advancing with the expanding scope of application and increase in global demand of PP. Along with PP materials, plastic materials are also being used increasingly in automobile parts, and many automotive resin parts are microprocessed (emboss processed) in injection molding dies for improving their decorativeness and functionality. Micromolding technology based on injection molding has also been developed to form microstructures of various patterns on the surface of molded articles. Since the publication of related papers in 1996,

several researchers have focused on microinjection molding, and extensive investigations are still being conducted. From the viewpoint of the micromolding technology in injection molding, a great variety of plastic molded articles having submicron scale surface structures have already been developed, including, as a representative example, the optical disk. Recently, for digital versatile disks (DVDs), Blu-ray DVDs, and similar products, this has become a technically matured precision transfer molding technology. Consequently, several discussions concerning the surface transferability and moldability have been conducted [2–5]. Previously, the relation between the material properties and transferability has been discussed based on the viscosity of the molten resin, change in storage modulus of the cooling resin produced in the mold, and transfer mechanism due to the deformation of skin and shear layer [6–8]. In general-purpose injection molding, a high transfer rate is shown for 36- $\mu\text{m}$ -deep cavity having a 200–300- $\mu\text{m}$ -diameter arc [9], but the critical domain of filling into a conic recession is about  $\Phi 10 \mu\text{m}$  [10, 11]. Therefore, to form finer structures, suitable techniques have been developed to delay the solidification speed of the resin and complete the transfer before solidification. Researches on ultra-high-speed injection molding, injection compression molding, in-mold pressure reduction, high-temperature die molding, CO<sub>2</sub> gas injection molding, ultrasonic vibration molding, among other approaches, have been reported to improve transfer in existing technologies [12–18]. To visualize the filling pattern of V-grooves in ultra-high-speed injection molding, Yokoi et al. reported the effect of injection rate on transfer [19]. Changes in transfer rate due to the installation of stamper grooves and impact of the filling rate and in-mold pressure were examined in detail. From the viewpoint of bonding, Ito et al. reported resin–metal bonding using processing technology that produces a fine structure on the metal surface [20–23]. From the viewpoint of controlling microstructures at the resin interface, researches have been conducted on the water repellency of microstructures [24–26]. Till date, majority of research on micromolding in injection molding has been focused on amorphous materials; however, in recent years, researches using crystalline resin materials have also expanded steadily [27, 28]. Jiang et al. produced PP macrogears, and they performed structural analysis and evaluated their surface dynamical properties by nanoindentation [29]. Furthermore, Babenko et al. evaluated the heat transfer coefficient of PP and molds in microinjection molding by experiments and simulations [30]. Kazema et al. demonstrated the impact of internal structure and crystallization of PP on transfer processes [31, 32]. Furthermore, Takai et al. evaluated the influence of molecular structure and viscosity of PP on microtransfer and reported that low strain fluidity may be attributed to the transfer rate [33]. However, although there are reports on

Correspondence to: S. Kuroda; e-mail: shinichikuroda@mail.nissan.co.jp

DOI 10.1002/pen.25266

Published online in Wiley Online Library (wileyonlinelibrary.com).

© 2019 Society of Plastics Engineers

microtransferability by injection molding using crystalline resin material, that is, PP, the effects of materials containing talc or rubber that are blended with PP on microtransfer has not been investigated sufficiently.

Currently, there is an increase in the need to reduce the gloss level of resin surfaces and obtain a matte feeling that improves the surface texture of automotive parts. Studies have been conducted to quantify the effects that visually influence the gloss level [34, 35]. To obtain a product surface having low gloss value, precise transfer of a microstructure with several micrometers of unevenness on the mold surface is necessary. Talc and rubber components with particle sizes of several micrometers blended in PP can be assumed to have an effect on this fine transfer. Therefore, understanding the effect of talc and rubber components blended in PP on surface transfer processes can be assumed to contribute both to an enhanced texture and diminishing of the transfer defects that occur during mass production. This should impart more advanced decoration and functionality. In previous research, we focused on the microstructure transfer of talc- and rubber-containing PP resin materials that are widely used in automobiles and examined the impact of the amount of talc and rubber and of their detailed components on the transfer process [36]. According to the generally adopted opinion, to achieve a fine uneven shape, the mold must be subjected to microprocessing whereby its shape is accurately transferred [12–18]. However, since it was also found that the self-formation of fine irregularities occurs in talc-containing PP as a consequence of PP shrinkage in the untransferred region, the self-formation of fine irregularities was suggested to be a new transfer mechanism for crystalline PP materials for which achieving precise microtransfer is difficult. On the contrary, the effect of talc dispersibility and particle size on the self-formation of fine irregularities remained unknown in previous research, and the influence of self-formed unevenness on the final gloss level has not yet been clarified. Hence, this study aims to investigate the factors controlling self-formed microirregularities and elucidate the influence of self-formed microirregularities on the eventual gloss level. Thereafter, the relation between talc particle size and fine irregularities was investigated using materials having different talc particle sizes. We also examined the self-formed microirregularities and gloss level using micromold structures having different shapes.

## EXPERIMENTAL

### Material

Commercially available PP (Japan Polypropylene Corporation, NEWCON, NBX03HRS) was used for this study. The melt flow rate (MFR) was 30 g/10 min. Samples were produced using a base PP in the state before talc and rubber components were added and talc (Shiraishi Calcium Kaisha, Ltd., MAT-725TP and Nippon Talc Co., Ltd., PAOG-10, P-6). The average particle size of talc has changed at three levels in PP containing 20 wt% talc. To blend PP and talc, we used a coaxial twin-screw extruder (Toshiba Machine Co., Ltd., TEM35B) and manufactured the pallets with a screw rotational speed of 250 (rpm) with a cylinder temperature of 210°C–190°C.

### Mold

To examine the transferability of the vicinity of the gate and flow end part that may occur in the molded product, a test

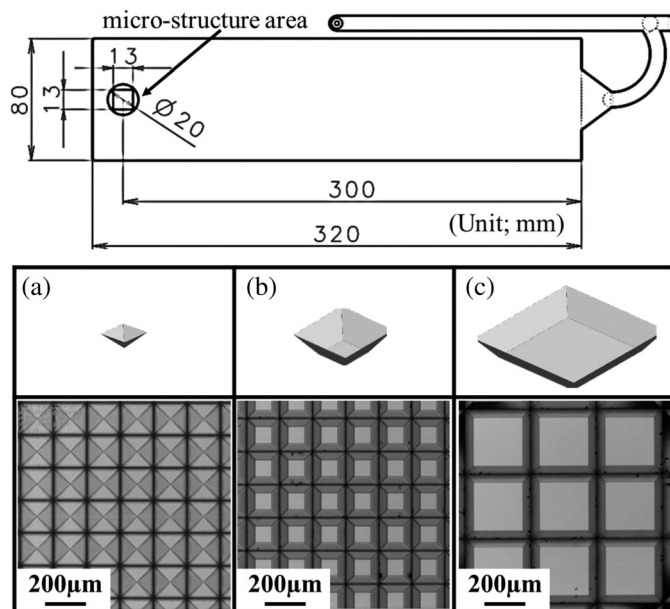


FIG. 1. Shape of molded samples and pictures of mold insert with micro-structure surface produced. (a) Pyramid shape, (b) trapezoid shape, (c) large trapezoidal shape of flat part.

specimen of  $320 \times 80$  mm and  $t = 2.5$  mm, as shown in Fig. 1, was used, and its transferability was evaluated at a position 300 mm away from the gate. In practical automotive bumper injection molding, the flow length from one gate is often in the order of 300 mm. Herein, we selected an area with decreased filling pressure for evaluation. The site of measurement was specified so that a plurality of patterns could be evaluated by a nesting exchange in nest-exchange mode. The mold material of the nest was 13Cr Mo-containing stainless steel, pre-hardened: 29–33 HRC (HPM38; Hitachi Steel Co., Ltd., Japan), and microfabrication was performed in the range of  $13 \times 13$  mm at the center of the nest.

Microprocessing of the mold surface produced three kinds of fine shapes. As a parameter for evaluating the shapes of irregularities, each characteristic micromorphology was taken as a shape varying the skewness  $R_{sk}$ , which expresses the extent of deviation in the height direction of the roughness curve.  $R_{sk}$  is a measure of the asymmetry of the probability density function in the height direction. A previous research has reported that the gloss level changes depending on the numerical value of  $R_{sk}$  [35]; however, previous evaluations were performed using a microprocessed mold based on the edging process, which is very likely to form unintended shapes. To accurately determine the transfer and non-transfer area herein, the microshape processing was performed using ultra-precision machining and nickel electrocasting, keeping in mind the typical shape and dimensions of emboss-processed-leather-like patterns that are widely used in automobiles. Herein, using this processing method, the molds of three different patterns with different  $R_{sk}$  were formed. Three types of microstructure patterns formed were referred to as A, B, and C. Pattern A was fabricated, as shown in Fig. 1a, with a repeating pyramid shape having side length and height of 200 and 100  $\mu\text{m}$ , respectively. As shown in Fig. 1b, pattern B had a trapezoidal shape with a height of 100  $\mu\text{m}$ , equivalent to that in A, and a flat surface of

200 × 200 μm on the top face. Since Rsk is an index that expresses the extent of deviation in the height direction of the cross-sectional curve, Pattern B shows a larger deviation than the pyramidal pattern A. As shown in Fig. 1c, Pattern C had a trapezoidal shape 100 μm in height, as in A, and a flat surface of 400 × 400 μm on the top face, which is larger than that of Pattern B. This indicates that the deviation of Rsk is even larger than that for Pattern B. Molding experiments were performed using molds with these three different levels of Rsk.

#### Injection Molding Machine and Molding Conditions

For molding, a 110 t injection molding machine (Nissei Resin Industry Co., Ltd., FN 2000-25A) was used. The maximum injection speed was 100 mm/s, highest injection pressure was 220 MPa, clamping force was 1,098 kN, and screw diameter was 35 mm. Molding conditions were set to injection conditions assuming general molding conditions for automotive resin parts, including an injection speed of 50 mm/s, holding pressure of 20 MPa, resin temperature of 200°C, and mold temperature of 40°C. Each condition was set as an average condition for the bumper molding.

#### Measurement and Evaluation

Particle-size distribution was measured using a laser diffraction particle-size distribution analyzer (MASTERSIZER 3000; Malvern Instruments Ltd., UK) to measure the average particle size of talc at three levels, which was added in 20 wt%. To evaluate the impacts on flowability and crystalline state of the base PP and talc-containing PP materials, a dynamic viscoelasticity apparatus (RSA3; TA Instruments-Waters LLC, America) and differential scanning calorimeter (Q200; TA Instruments-Waters LLC, America) were used. Furthermore, to evaluate the wettability of the molten resin kneaded with talc to the mold, the contact angle between the melted resin and mold metal was determined using a contact angle meter (DM 501; Kyowa Interface Science Co., Ltd., Japan). The A mold with a pyramid-shaped pattern was used to analyze the molded articles composed of PP, to which talc of different average particle sizes was added. Furthermore, their transfer state and cross-sectional direction of the resin were determined with respect to the mold shape using laser microscopy (LEXT OLS 4100; OLYMPUS Corp., Japan) and scanning electron microscopy (SEM) (TM 3030 Plus; Hitachi High-Technologies Corp., Japan). Additionally, for the molds of Patterns A–C, the fine shape of the molded product with different particle sizes of talc was measured using a laser microscope, whereas the gloss level was evaluated using a glossmeter (GM-268 Plus; Konica Minolta Corp., Japan).

## RESULTS AND DISCUSSION

#### Average Particle Size of Talc

Figure 2 shows the average particle-size distribution of talc at three levels. According to the measurements, P-6 had the smallest average particle size of 4.0 μm, followed by MAT-725TP with an average particle size of 6.5 μm. PAOG-10 had the largest average particle size of 9.3 μm. Hereinafter, P-6, MAT-725TP, and PAOG-10 are described as an average particle diameter of 4.0, 6.5, and 9.3 μm, respectively. Furthermore, this three-level particle-size distribution showed the same normal portion, and it

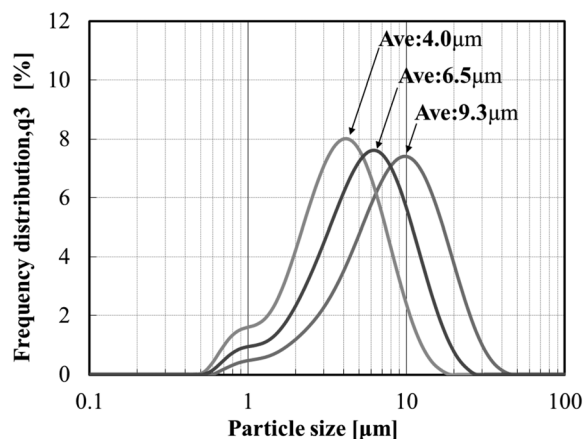


FIG. 2. Relation between average particle size and distribution.

could thus be confirmed that each average particle size showed a different particle size distribution for talc. Furthermore, these analyses demonstrated that talc having an average particle size of 9.3 μm contains talc with approximately 10% of particles exceeding 20 μm.

#### Effects of Talc Particle Size on Viscoelasticity and Transfer Height

Viscoelasticity was measured to determine how the flow phenomena of the resin during melting are affected by the incorporation of talc with different average particle size diameters. Results of these measurements are shown in Fig. 3. Previous studies have reported that resin microtransfer mainly occurs during the dwelling process [33]. Takai et al. studied the effect of viscosity on microtransfer during melting of PP and reported that resin materials having high fluidity at low strain suitable for dwelling processes exhibit improved transferability. Based on this, we consider the results of this experiment. The main conditions for the DMA analysis were as follows. Frequency: 6.283 (rad/s), geometry: rectangular (L = 38 mm, W = 6.2 mm, and T = 0.5) tension mode, experimental setup: strain 0.01 (%) and heating rate: 2 C/min. An analysis was performed with a furnace temperature of 40°C–170°C. According to the DMA results shown in Fig. 3, a general trend suggests that the storage modulus is higher due to the incorporation of talc into base PP. Furthermore, with an increase in average talc particle size, the storage modulus tended to increase with the highest level being obtained at an average particle size of 9.3 μm. On the contrary, when the resin temperature was above 165°C, the difference in storage modulus due to the difference in talc particle size was diminished. In addition, in the comparison of tan (delta), the difference between each sample was slight. It is thus assumed that the influence on the transferability during resin flow is small from the viewpoint of microtransfer, and there is apparently no significant difference in the range of talc particle size used herein. This indicates that with an increasing temperature, the storage elastic modulus of the base PP and that of the talc-containing PP become similar, suggesting that the base resin material becomes the dominant component during melting.

Figure 4 shows the results of measuring the transfer height (transfer rate) based on differences in the average particle size of talc at the three levels. Using the mold of Pattern A, the transfer height of the sample was measured with changing dwelling

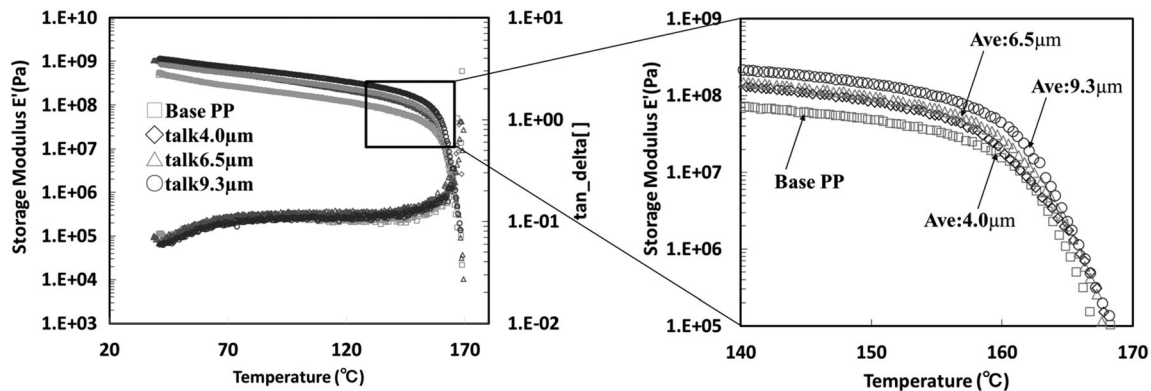


FIG. 3. Dynamic mechanical analysis data for Base PP, Talc content 20% average particle size 4.0  $\mu\text{m}$ , 6.5  $\mu\text{m}$ , and 9.3  $\mu\text{m}$ .

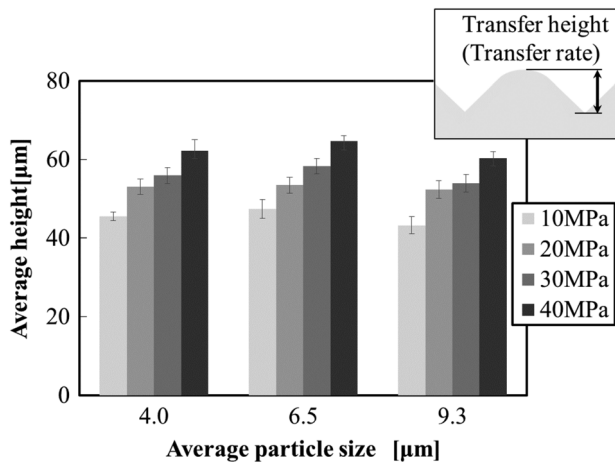


FIG. 4. Relation between average particle size and average height.

pressure: 10, 20, 30, and 40 MPa. According to the results of this measurement, no significant difference was observed in the transfer height due to differences in talc particle size. It can thus be confirmed that the differences in the talc particle size between the three levels, both as shown in this experiment and generally used for the evaluation of transferability, which hardly affect the viscoelasticity and transfer height.

#### Effects of Talc Particle Size on Crystallinity of Resin and Contact Angle with Mold

It is generally accepted that blending resin materials affects their degree of crystallinity. In this research, talc content was fixed

at 20 wt% in the base PP for the purpose of confirming whether the degree of crystallinity is affected by the inclusion of talc. To evaluate this, crystallinity was examined for the three talc particle diameters. According to the results of these analyses, the base PP demonstrated a mean crystallization rate of 33.0%, whereas the talc-included PP had an average crystallization rate of 33.1%. Therefore, no change was observed in the crystallization rate caused by including the talc. Furthermore, for the talc granule 3 standard, the crystallization rates per granule size of 4.0  $\mu\text{m}$  = 33.5%, 6.5  $\mu\text{m}$  = 32.5%, and 9.3  $\mu\text{m}$  = 33.1% were demonstrated, indicating that no significant difference was caused by granule size. Furthermore, for the talc granule 3 standard, the shrinkage rates per granule size of 4.0  $\mu\text{m}$  = 9.1/1,000, 6.5  $\mu\text{m}$  = 9.4/1,000, and 9.3  $\mu\text{m}$  = 8.9/1,000 were demonstrated, indicating that no significant difference was caused by granule size. Subsequently, contact angle the molten resin and mold metal was analyzed to clarify the effect of talc particle size on the contact angle. A given amount of PP resin was dropped onto a metal plate made of the same material as the mold and heated to 200°C, and the contact angle of the metal plate and resin was measured in a sufficiently molten state. As shown in Fig. 5, the analysis results indicate that the case of the talc-containing PP compared with the base PP showed an increase and decrease in the contact angle and wettability, respectively. As suggested from the results shown in the DMA analysis described in the previous section, this can be attributed to the general tendency for suppression of the deformation of resin materials with the inclusion of talc. On the contrary, due to the difference in the talc particle size, the contact angle showed a slight increase with increasing average particle size, but this was not significant considering the overall dispersion of data. We can thus conclude

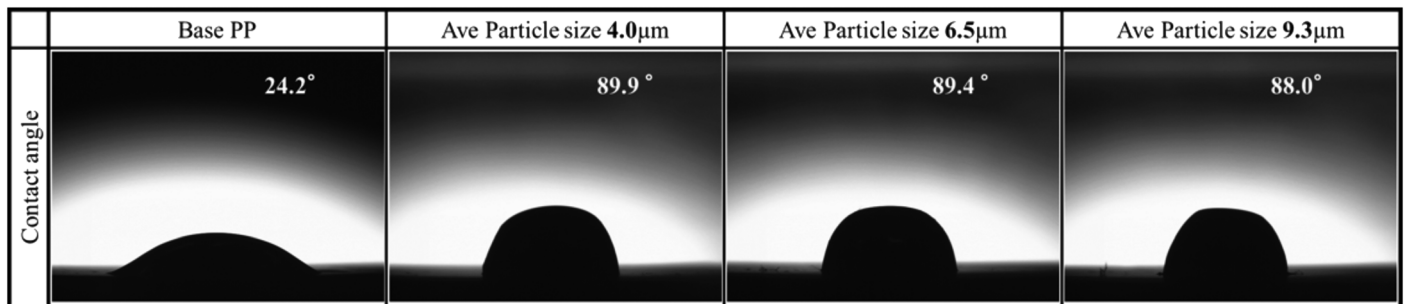


FIG. 5. Effect of added talc average particle size on contact angle between melted PP and mold wall.

that although the degree of crystallinity and wettability decreases after the inclusion of talc, when the average particle diameter of talc is in the range of 4.0–9.3  $\mu\text{m}$ , the difference in crystallinity degree and wettability with the mold in the molten state is not significant.

#### Effect of Talc Particle Size on Microtransfer

Next, using talc-containing materials with the three different levels of the average particle size, we performed molding experiments using the mold with Pattern A to investigate the effect of the talc particle size on the formation of microirregularities self-formed by talc. Figure 6 shows the results of laser microscope observation near the top of the pyramid of the formed sample. In the untransferred area near the top of the pyramid, microirregularities of several micrometers were formed irrespective of the average particle size of talc. On the contrary, in the molded product with the average particle diameter of talc of 9.3  $\mu\text{m}$ , the pyramid shape of the untransferred area was distorted, and microirregularities of several micrometers were also observed. Furthermore, when observing the continuous cross-sectional shape distribution of the pyramidal shape, a deformation of approximately 10–20  $\mu\text{m}$  was noted. To analyze this deformation factor in more detail, the vicinity of the top of pyramid was cut parallel to the flow direction, and the cross section was observed by SEM. Figure 7 shows the results of cross-sectional observation. For all average particle sizes of talc, it was observed that talc was distributed near the skin layer at the top of the pyramid. However, although talc was evenly distributed in molded items with the average particle diameter of 4.0  $\mu\text{m}$ , talc of approximately 20- $\mu\text{m}$  diameter was scattered near the top of the pyramid in the molded item of 9.3- $\mu\text{m}$  diameter and talc was present immediately below

the site where the pyramid shape was deformed. Upon observing the talc under higher magnification, it was found that talc of approximately 20  $\mu\text{m}$  served as the nucleating agent, and fine talc of several  $\mu\text{m}$  was aggregated. This is because, as described in the analysis of Section Average particle size of talc, talc having the average particle diameter of 9.3  $\mu\text{m}$  contains approximately 10% of talc exceeding 20- $\mu\text{m}$  diameter, and this large talc becomes the nucleus for the aggregation of fine talc, whereby a larger lump of talc appears to be distributed near the surface layer of the pyramid. Thus, we can infer that a region having few talc particles was formed around the aggregated talc, and a deformation of approximately 10–20  $\mu\text{m}$  was generated in the shrinking process of the base PP due to the density differences in the talc distribution. This phenomenon is difficult to explain in terms of the viscoelasticity or transfer height (transfer rate), which are conventionally used as indicators for evaluating the transfer. As described in Section Effects of talc particle size on viscoelasticity and transfer height, it can be confirmed that the difference in the average particle size of talc had little effect on these indicators but rather exerted a significant effect on the self-formation of microirregularities. On the contrary, there is a possibility that the self-formed microshape could be controlled by the talc particle size. Consequently, the development of a new transfer technology is expected, resulting in a different microtransfer technology compared with that applied previously and that entirely transfers the mold shape.

#### Influence of the Untransferred Area on Microtransfer

To clarify the influence of the change in the untransferred area on the self-formation of microirregularities, molding experiments were performed using molds with different microstructures. The

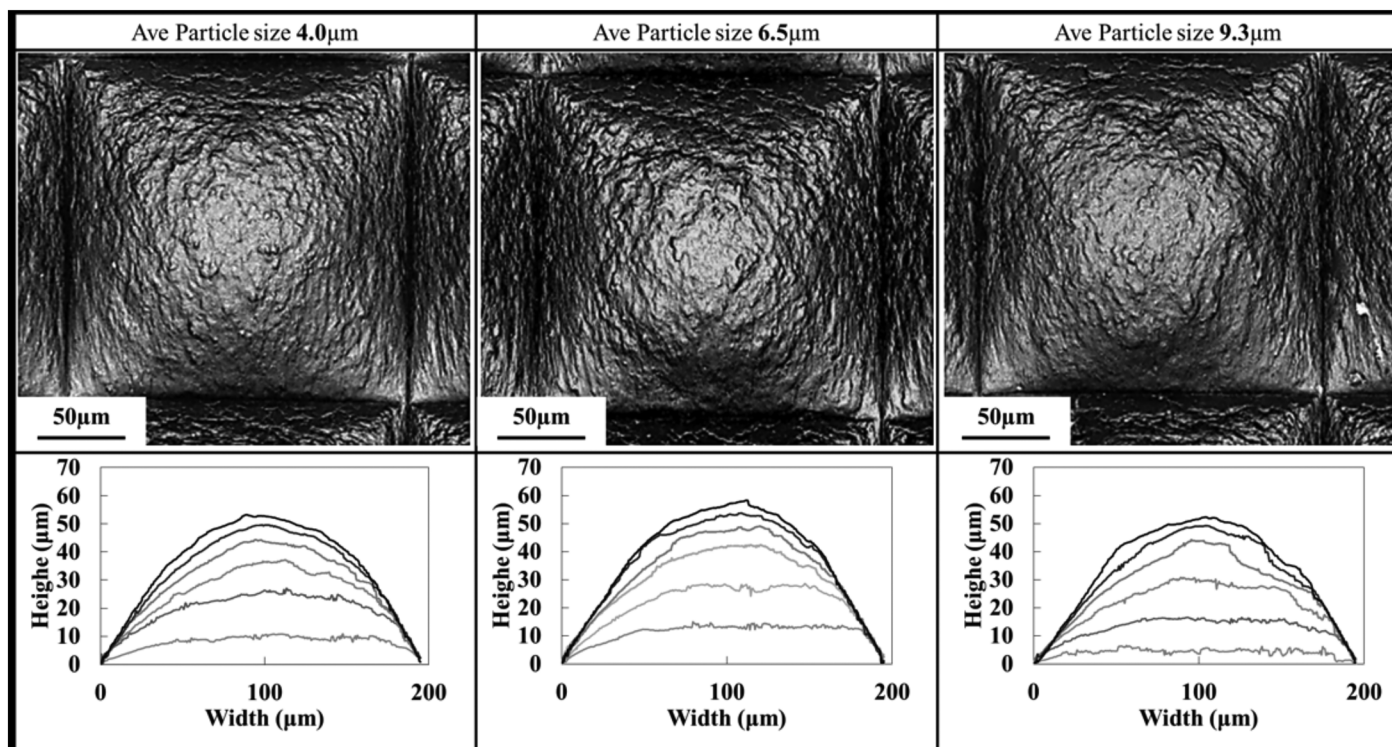


FIG. 6. Effect of talc average particle size on transcribed shape's height and surface.

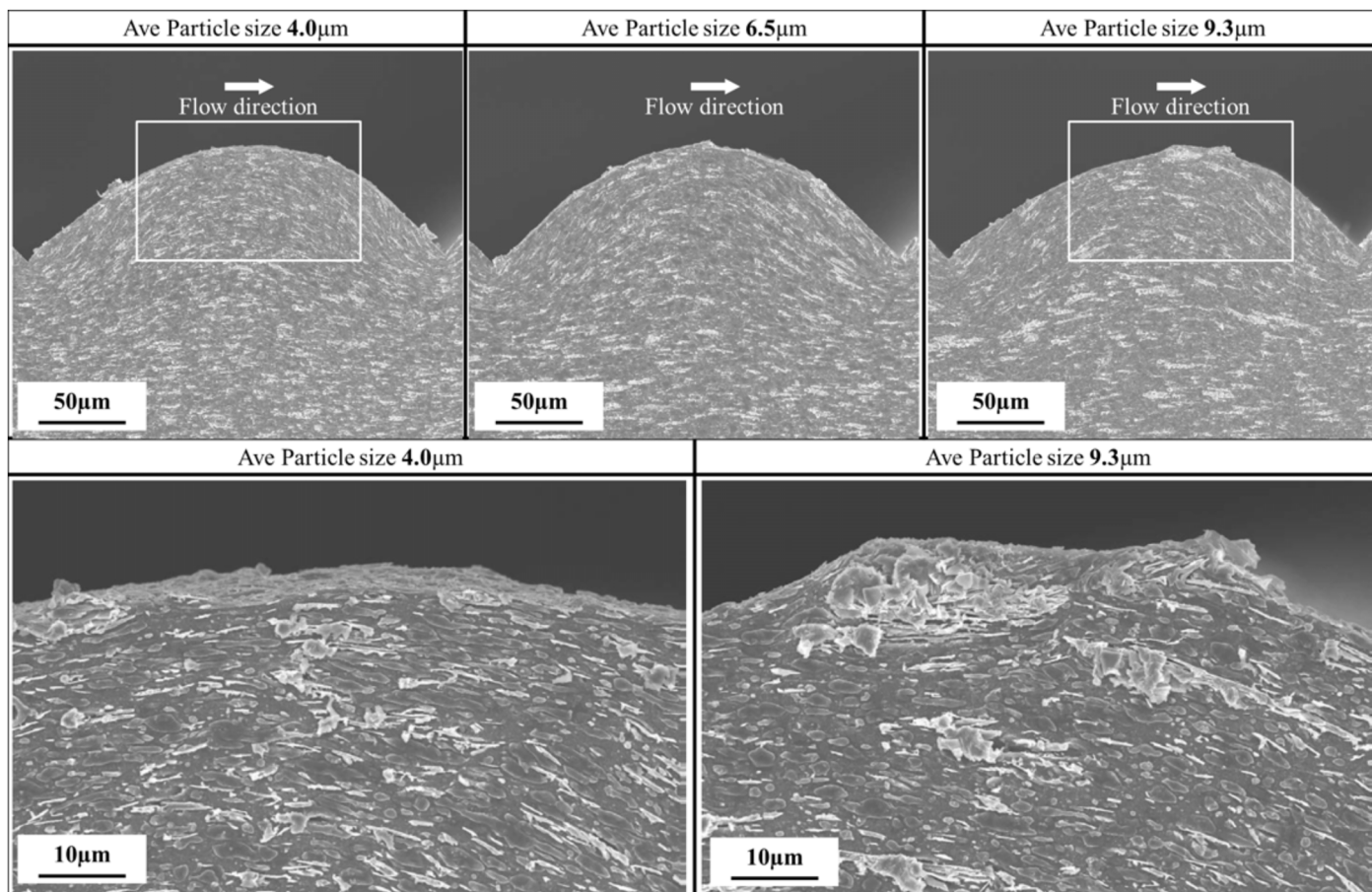


FIG. 7. Effect of talc distribution on transcribed shape height.

mold used in this experiment had varying  $R_{sk}$ , which represents the degree of deviation in the height direction of the roughness curve, as a result of the change in the pattern of the microstructure. Previous study has reported the influence of  $R_{sk}$  on the gloss level [35], that is, the gloss value increases as the deviation in  $R_{sk}$  increases (when the area of the flat portion increases). In the present research, molding experiments were conducted using the three different levels of the microstructural Patterns A, B, and C with different  $R_{sk}$  values with varying flat areas, as shown in Fig. 1, and investigations were conducted on microstructures that are self-formed under the influence of talc. Figure 8 shows the results of laser microscope observation of molded articles containing the average talc particle sizes of 4.0, 6.5, and 9.3  $\mu\text{m}$  in the base PP, obtained in the respective microstructured dies of Patterns A, B, and C. According to these results, as was observed in the case of Pattern A, Patterns B and C exhibited self-formed microstructures near their tops. On the contrary, it was confirmed that in the talc-free base PP, the microirregularities observed in the talc-containing material were not formed in the untransferred area near the top. A characteristic distribution was observed in Pattern C, as shown in Fig. 9. This fine tiger-stripe pattern with a depth of several tens of  $\mu\text{m}$  occurred in the direction transversal to the flow direction. This phenomenon was most remarkable in talc-containing materials with the average particle diameter of 9.3  $\mu\text{m}$  but was also detectable in the base PP. In other words, because of the occurrence regardless of the talc content, it can be assumed that once the resin is transferred in the microstructure of

the mold, the phenomenon is due to the deformation of the microstructure of the molded article in the process of causing the PP material to shrink in the mold. Meanwhile, the reason for which the fine tiger-stripe pattern increased with larger average particle size of talc can be probably explained by the dispersion of talc, as mentioned in Section Effect of talc particle size on microtransfer, keeping in mind the impact of crystallinity and wettability due to differences in the average particle size, as described in Section Effects of talc particle size on crystallinity of resin and contact angle with mold. Where the average talc particle size is larger, the aggregation of talc is enhanced, and considering that density difference in the talc distribution suppresses deformation and shrinkage in the high-density area. Since deformation and shrinkage occurs in the low-density area, it can be inferred that the fine tiger-stripe pattern was more notable in the material with a large average particle diameter of talc. Furthermore, the fact that fine tiger-stripe pattern is more significant in the Pattern C than that A and B is probably due to more intensive resin inflow as the area of the plane portion is expanded in the Pattern C.

#### *Effects of $R_{sk}$ and Talc Average Particle Size on Gloss Level*

Next, to examine the effect of the self-formed microstructure on the gloss level of the final product, the gloss values of the molded articles of the microstructure Patterns A, B, and C with different  $R_{sk}$  were measured. To elucidate the effect of microstructure on the gloss level, the gloss was measured using the

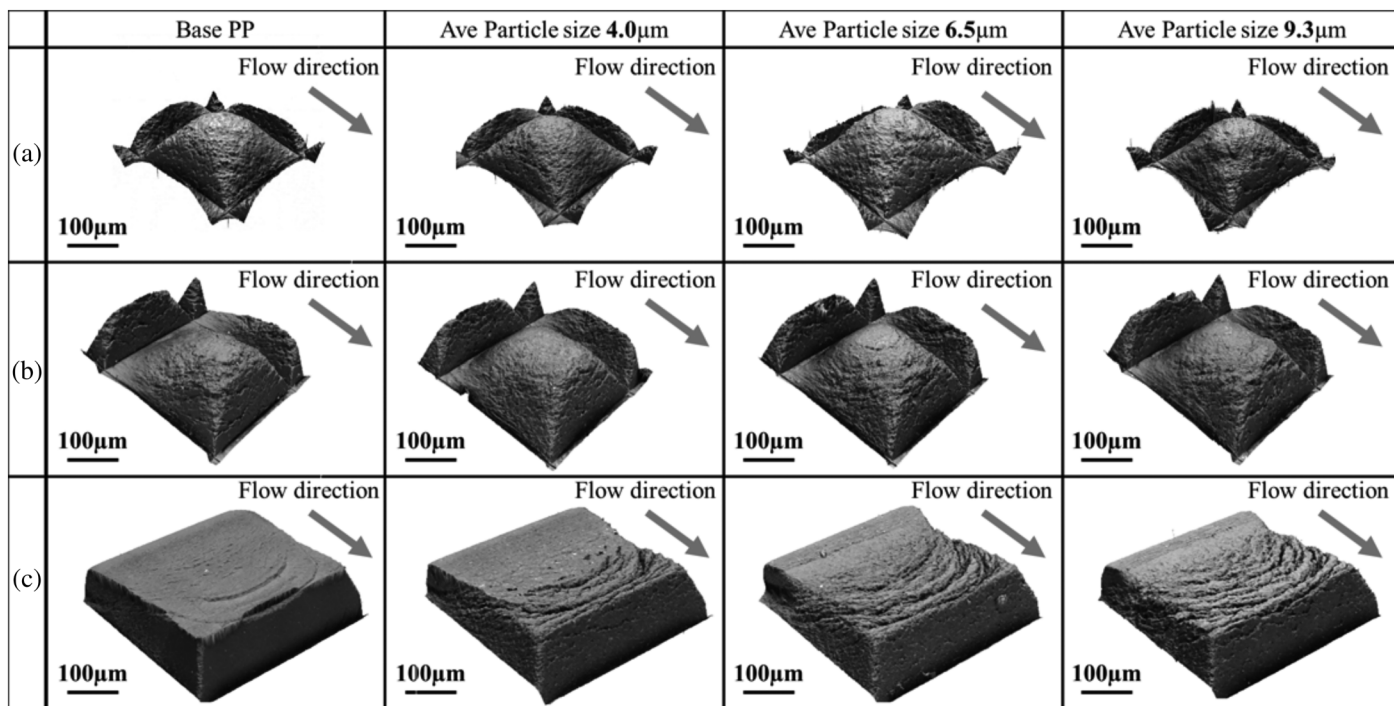


FIG. 8. Effect of Rak and talc average particle size on transcribed shape's height and surface.

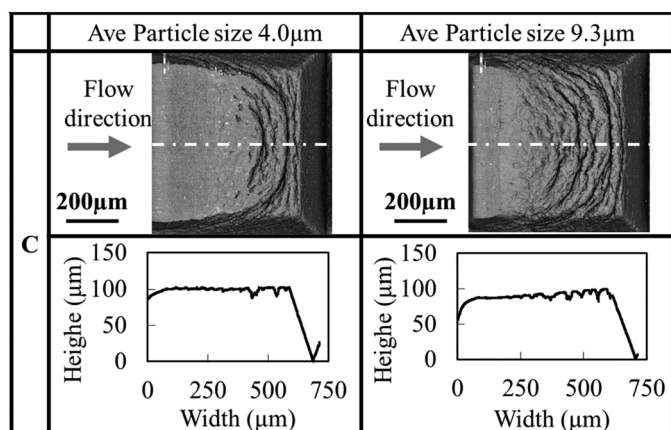


FIG. 9. Effect of talc average particle size on transcribed shape surface pattern.

same samples as those used to analyze the microstructure in Section Influence of the untransferred area on microtransfer. Results of measurement are shown in Fig. 10. As in previous research, the gloss value increased with increasing deviation of Rsk in the negative direction. The deviation in Rsk shows the expansion of the area of the flat surface, and it can be inferred that, when measuring the gloss to evaluate the light reflectance, light reflectance increases due to the expansion of the flat surface. On the contrary, compared with base PP, the gloss value decreased in molded samples containing talc with large average talc particle diameter, which is particularly notable in the microstructural pattern C. This is considered to be due to the fine tiger-stripe pattern described in Section Influence of the untransferred area on microtransfer. The fine design observed in Pattern C has a

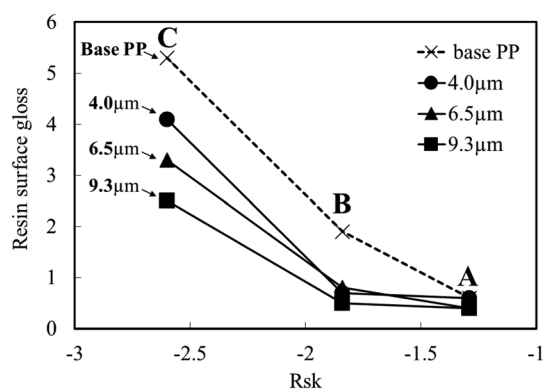


FIG. 10. Relation between average Rsk and resin surface gloss.

depth of up to several tens of  $\mu\text{m}$ , and it can be supposed that the gloss level decreased due to diffused light reflection caused by a better-expressed tiger-stripe pattern together with the expansion of the average particle diameter.

## CONCLUSIONS

- The impact of the change in talc content and average particle diameter of talc in the PP resin on transferability and gloss level were qualitatively and quantitatively presented.
- With the incorporation of talc, microirregularities of approximately several micrometers were self-formed by the shrinkage of PP in the untransferred region. Furthermore, the self-formed unevenness became more significant with an increase in the average particle diameter of talc. In particular, the addition of talc with a particle diameter of  $20\ \mu\text{m}$  or more causes a deformation of approximately several tens of  $\mu\text{m}$  to  $20\ \mu\text{m}$ .

• It was observed that a fine tiger-stripe pattern due to in-mold shrinkage and density differences in talc was formed in the untransferred area of the flat part along with an increase in the Rsk deviation, which is an index showing the bias of mold irregularities.

• The gloss level increased with an increase in the Rsk deviation but decreased with increasing average particle size of talc. A plausible reason for this is that the diffuse reflection of light is increased by the microirregularities formed in the untransferred area.

• In the past, the gloss level was controlled by changing the microstructure of the mold and accurately transferring the shape of the mold. This study demonstrated that the gloss level of the product changes due to the microirregularities that talc produces by self-formation, and highlights the unrecognized possibility that this change can be controlled by the average particle diameter of talc and the structure of the mold.

### Abbreviations

PP	polypropylene
MFR	melt flow rate
SEM	scanning electron microscope
DMA	dynamic mechanical analyzer
DSC	differential scanning calorimetry

### REFERENCES AND CITED WORK

1. T. Nomura, T. Nishio, T. Sato, and H. Sano, *Polym. Sci. Tech.*, **50**, 81 (1993).
2. M. Yoshii, H. Kuramoto, and K. Kato, *Polym. Eng. Sci.*, **33**, 1251 (1993).
3. M. Yoshi and N. Ebinuma, *JSPP*, **6**, 90 (1994).
4. M. Hirata, H. Kitamura, and Y. Kinugasa, *JSPP*, **10**, 129 (2000).
5. Y. Ootera, *JSPP*, **17**, 384 (2005).
6. M. Ueda, *JSPP*, **13**, 732 (2001).
7. M. Yoshii, H. Kuramoto, and Y. Ochiai, *Polym. Eng. Sci.*, **38**, 1587 (1998).
8. T. Yasuhara, K. Kato, H. Imamura, and N. Otake, *JSPP*, **43**, 492 (2002).
9. Y.H. Lin, C.F. Huang, H.C. Cheng, Y. Lin, J.L. Lee, and Y. K. Shen, *Polym. Eng. Sci.*, **53**, 212 (2012).
10. K. Sato, K. Miyaguchi, and H. Saito, *Indus. Res. Inst. Niigata Prefect.*, **38**, 45 (2008).
11. T. Kato, *Fabric. Mater.*, **50**, 3 (2009).
12. E. Yasuhara, K. Sawamoto, K. Kato, and N. Otake, *Proc. Joint. Tech. Plas.*, **54**, 319 (2004).
13. H. Yokoi and A. Oomori, *JSPP*, **17**, 3 (2006).
14. M. Yoshii, H. Kuramoto, and Y. Ochiai, *Polym. Eng. Sci.*, **34**, 1211 (1994).
15. E. Monkkonen, T.T. Pakkanen, T. Hietala, and T. Kaikuranta, *Polym. Eng. Sci.*, **42**, 1600 (2002).
16. M. Choi, N. Lee, J. Hang, and S. Kang, *ANTEC. Proc.*, **4**, 2018 (2007).
17. S.C. Tseng, Y.C. Chen, C.H. Lin, B.Y. Shew, and L.C. Kuo, *Int. Polym. Process.*, **21**, 340 (2006).
18. T. Katoh, R. Tokuno, Y. Zhang, M. Abe, and M. Akamatsu, *Microsyst. Technol.*, **14**, 1507 (2008).
19. X. Ham, H. Yokoi, and T. Takahashi, *Int. Polym. Process.*, **21**, 473 (2006).
20. H. Ito, K. Kazama, T. Yasuhara, T. Saito, and T. Kikutani, *Polym. Sci.*, **22**, 6 (2006).
21. K. Ohnami, T. Takayama, K. Taki, D. Funaoka, and H. Ito, *IUPAC Macro. Pro.*, **18**, 326 (2014).
22. E. Muraoka, H. Ito, H. Ooshima, and T. Adachi, *JSPP*, **15**, E-205 (2015).
23. E. Muraoka, H. Ito, T. Takayama, and H. Ooshima, *Adachi T. JSPP*, **14**, 323 (2014).
24. D. Chu, A. Nemoto, and H. Ito, *Microsyst. Technol.*, **20**, 193 (2014).
25. D. Chu, A. Nemoto, and H. Ito, *Appl. Surf. Sci.*, **300**, 117 (2014).
26. D. Chu, A. Nemoto, and H. Ito, *Microsyst. Technol.*, **21**, 123 (2015).
27. Y. Takei, *Polym. Preprints. Japan.*, **62**, 2112 (2013).
28. E. Yanagisawa and T. Tkatuji, *Trans. Jpn. Sci. Mech. Eng.*, **79**, 807 (2013).
29. J. Jiang, S. Wang, B. Suna, S. Ma, J. Zhang, Q. Li, and G.H. Hu, *Mater. Des.*, **88**, 245 (2015).
30. M. Babenko, J. Sweeney, P. Petkov, F. Lacan, and B. Whiteside, *Appl. Therm. Eng.*, **130**, 865 (2018).
31. H. Ito, K. Kazama, and T. Kikutani, *Macromol. Symp.*, **628**, 249 (2007).
32. K. Taki, S. Nakamura, T. Takayama, A. Nemoto, and H. Ito, *Microsyst. Technol.*, **22**, 31 (2016).
33. Y. Takai, T. Takayama, K. Taki, H. Ito, A. Takai, and S. Sonobe, *AWPP2014*, **1116**, 17 (2014).
34. P.L. Menezes, S. Kishore, V. Kailas, and M.R. Lovell, *Wear*, **271**, 2213 (2011).
35. M. Yonehara, J. Tatsuno, H. Nakamura, and S. Takehara, *Annual Report of Fundamental Technology for Next Generation Research Institute, Kindai University*, **3**, 73 (2012).
36. S. Kuroda, A. Mizutani, and H. Ito, *J. Polym. Eng.*, **39**, 299 (2018).